ÉCOLE POLYTECHNIQUE
FÉDÉRALE DE LAUSANNE

HARVARD
MEDICAL SCHOOL

REGULARIZED SPATIOTEMPORAL DECONVOLUTION OF fMRI DATA USING GRAY-MATTER CONSTRAINED TOTAL VARIATION

Younes Farouj, F. Işık Karahanoğlu and Dimitri Van De Ville

IEEE International Symposium on Biomedical Imaging
Melbourne, April 20, 2017

In just one slide

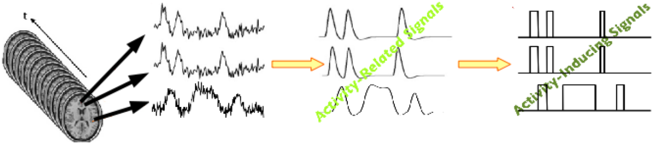

fMRI time series (indirect measures of neuronal activity)

The observed signal $\mathbf{y}$ (3D+t) is a noisy version of the BOLD response $\mathbf{x}(t)$ (activity related signal):

$$\mathbf{y} = \mathbf{x} + \varepsilon.$$

Random noise and nuisance components (fluctuations, signal drift, residual errors from motion correction, etc $\cdots$) $\Longrightarrow$ Very low signal-to-noise ratio.

In just one slide

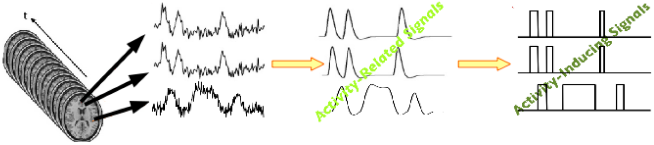

fMRI time series (indirect measures of neuronal activity)

The observed signal $\mathbf{y}$ (3D$+t$) is a noisy version of the BOLD response $\mathbf{x}(t)$ (activity related signal):

$$\mathbf{y} = \mathbf{x} + \varepsilon.$$

Random noise and nuisance components (fluctuations, signal drift, residual errors from motion correction, etc $\cdots$) $\Longrightarrow$ Very low signal-to-noise ratio.

Aim: Uncover the underlying activity from corrupted observations (preprocessing).

In just one slide

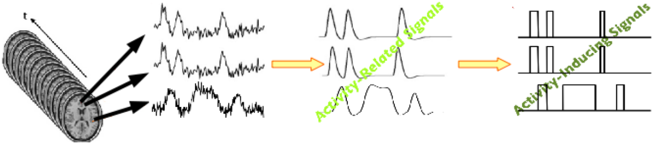

fMRI time series (indirect measures of neuronal activity)

The observed signal $\mathbf{y}$ (3D+t) is a noisy version of the BOLD response $\mathbf{x}(t)$ (activity related signal):

$$\mathbf{y} = \mathbf{x} + \varepsilon.$$

Random noise and nuisance components (fluctuations, signal drift, residual errors from motion correction, etc $\cdots$) $\Longrightarrow$ Very low signal-to-noise ratio.

Aim: Uncover the underlying activity from corrupted observations (preprocessing).

$\longrightarrow$ Without knowledge about timing, duration or position of neuronal events (spontaneous and resting-state activity).

BOLD modeling

- Temporal modeling:

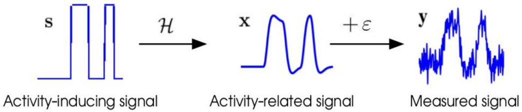

$\mathcal{H}$: Linear Translation Invariant system describing the response of the neuronal system (hemodynamic response function).

BOLD modeling

- Temporal modeling:

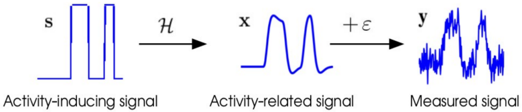

$\mathcal{H}$: Linear Translation Invariant system describing the response of the neuronal system (hemodynamic response function).

- Spatial modeling: Neurons are not activated individually; clustered localized regions are evoked

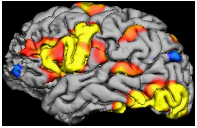

BOLD modeling

- Temporal modeling:

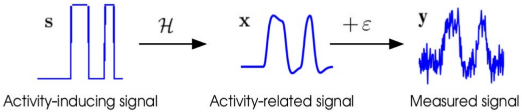

$\mathcal{H}$: Linear Translation Invariant system describing the response of the neuronal system (hemodynamic response function).

- Spatial modeling: Neurons are not activated individually; clustered localized regions are evoked

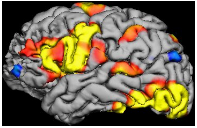

$\longrightarrow$ Use of an adapted total variation.

fMRI Analysis

- Generalized Linear Models (most commonly used) .

fMRI Analysis

- Generalized Linear Models (most commonly used) .
- Deconvolution techniques (for exploring spontaneous activity / resting-state networks) [Gaudes-Caballero et al. 2011].

fMRI Analysis

- Generalized Linear Models (most commonly used) .
- Deconvolution techniques (for exploring spontaneous activity / resting-state networks) [Gaudes-Caballero et al. 2011].

- Spatio-temporal deconvolution (More robust: Takes into account spatial and temporal properties) $\longrightarrow$ total activation (TA) of [Karahanoğlu et al. 2013].

$$\widehat{\mathbf{x}} = \arg\min_{\mathbf{x}} \left\{ \frac{1}{2} ||\mathbf{y} - \mathbf{x}||_2^2 + \mathcal{R}_T(\mathbf{x}) + \mathcal{R}_S(\mathbf{x}) \right\}.$$

$\mathcal{R}_T$: Generalized total variation.
$\mathcal{R}_S$: ℓ_2-smoothness within regions predefined by an atlas.

fMRI Analysis

- Generalized Linear Models (most commonly used) .
- Deconvolution techniques (for exploring spontaneous activity / resting-state networks) [Gaudes-Caballero et al. 2011].

- Spatio-temporal deconvolution (More robust: Takes into account spatial and temporal properties) $\longrightarrow$ total activation (TA) of [Karahanoğlu et al. 2013].

$$\widehat{\mathbf{x}} = \arg\min_{\mathbf{x}} \left\{ \frac{1}{2} ||\mathbf{y} - \mathbf{x}||_2^2 + \mathcal{R}_T(\mathbf{x}) + \mathcal{R}_S(\mathbf{x}) \right\}.$$

$\mathcal{R}_T$: Generalized total variation.
$\mathcal{R}_S$: ℓ_2-smoothness within regions predefined by an atlas.

Our proposal: Construct a method that is not biased by atlas-based partitioning of the brain (extension of TA).

Proposed framework

- Temporal regularization $\mathcal{R}_T$:

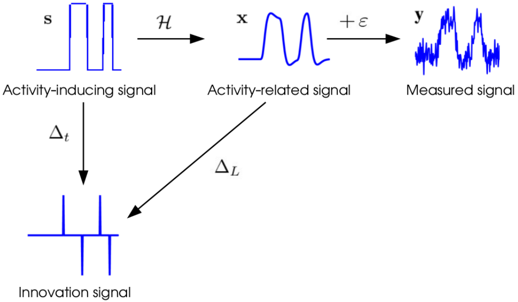

Δ_t: Temporal finite difference operator.
The activity-inducing signal $\mathbf{s}$ is block-type $\Longrightarrow$ $\Delta_t\{\mathbf{s}\}$ is a sparse (innovation) signal.
This suggests using $TV\{\mathbf{s}\} = ||\Delta_t\{\mathbf{s}\}||_1$ as a regularizer.

Proposed framework

- Temporal regularization $\mathcal{R}_T$:

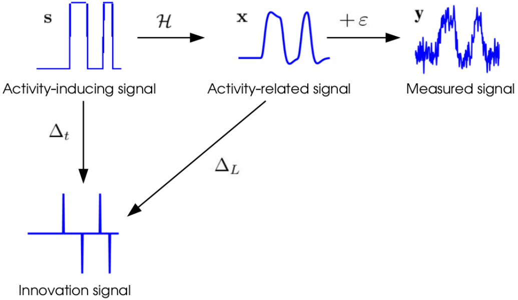

Δ_t: Temporal finite difference operator.
The activity-inducing signal $\mathbf{s}$ is block-type $\Longrightarrow$ $\Delta_t\{\mathbf{s}\}$ is a sparse (innovation) signal.
This suggests using $TV\{\mathbf{s}\} = ||\Delta_t\{\mathbf{s}\}||_1$ as a regularizer.
The BOLD signal $\mathbf{x}$ is given as $\mathbf{s}$ under the action of $\mathcal{H}$
$\Longrightarrow$ Sparsify $\mathbf{x}$: $\Delta_L\{\mathbf{x}\}$, with $\Delta_L = \Delta_t \mathcal{H}^{-1}$.

Proposed framework

- Temporal regularization $\mathcal{R}_T$:

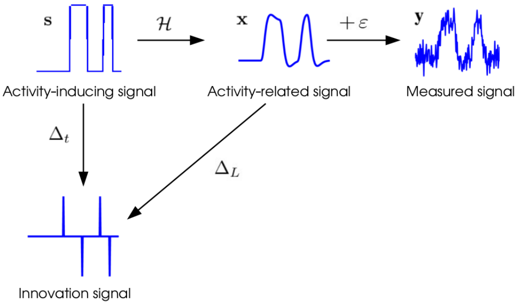

Δ_t: Temporal finite difference operator.
The activity-inducing signal $\mathbf{s}$ is block-type $\Longrightarrow$ $\Delta_t\{\mathbf{s}\}$ is a sparse (innovation) signal.
This suggests using $TV\{\mathbf{s}\} = ||\Delta_t\{\mathbf{s}\}||_1$ as a regularizer.
The BOLD signal $\mathbf{x}$ is given as $\mathbf{s}$ under the action of $\mathcal{H}$
$\Longrightarrow$ Sparsify $\mathbf{x}$: $\Delta_L\{\mathbf{x}\}$, with $\Delta_L = \Delta_t\mathcal{H}^{-1}$.
$\Longrightarrow$ Generalized TV (GTV) of [Karahanoğlu et al. 2011]

$\mathcal{H}$ can be elegantly described as a differential operator [Khalidov et al. 2011]:

$$\mathcal{H} = \frac{D - \gamma I}{\prod_{i=1}^{4}(D - \alpha_i I)}, \qquad \text{D : Temporal derivative.}$$

$\mathcal{H}$ can be elegantly described as a differential operator [Khalidov et al. 2011]:

$$\mathcal{H} = \frac{D - \gamma I}{\prod_{i=1}^{4}(D - \alpha_i I)}, \qquad \text{D : Temporal derivative.}$$

$\Longrightarrow$ Impulse response h characterized by 4 poles and 1 zeros:

$$\widehat{h} = \frac{j\omega - \gamma}{\prod_{i=1}^{4}(j\omega - \alpha_i)}$$

$\mathcal{H}$ can be elegantly described as a differential operator [Khalidov et al. 2011]:

$$\mathcal{H} = \frac{D - \gamma I}{\prod_{i=1}^{4}(D - \alpha_i I)}, \qquad \text{D : Temporal derivative.}$$

$\Longrightarrow$ Impulse response h characterized by 4 poles and 1 zeros:

$$\widehat{h} = \frac{j\omega - \gamma}{\prod_{i=1}^{4}(j\omega - \alpha_i)}$$

$\longrightarrow$ To compute $\Delta_L = \Delta_t \mathcal{H}^{-1}$, add a zero at the origin.

$$\Delta_L = \frac{D \prod_{i=1}^{4}(D - \alpha_i I)}{D - \gamma I}$$

$\mathcal{H}$ can be elegantly described as a differential operator [Khalidov et al. 2011]:

$$\mathcal{H} = \frac{D - \gamma I}{\prod_{i=1}^{4}(D - \alpha_i I)}, \qquad \text{D : Temporal derivative.}$$

$\Longrightarrow$ Impulse response h characterized by 4 poles and 1 zeros:

$$\widehat{h} = \frac{j\omega - \gamma}{\prod_{i=1}^{4}(j\omega - \alpha_i)}$$

$\longrightarrow$ To compute $\Delta_L = \Delta_t \mathcal{H}^{-1}$, add a zero at the origin.

$$\Delta_L = \frac{D \prod_{i=1}^{4}(D - \alpha_i I)}{D - \gamma I}$$

- Remember this regularization should be applied for all voxel:

$$\mathcal{R}_T(\mathbf{x}) = \sum_{v=1}^{N_x} \lambda_T(v) \, ||\Delta_L\{\mathbf{x}\}[v]||_1,$$

N_x: number of voxels and $\lambda_T(v)$ temporal regularization parameter for voxel v.

- Spatial regularization $\mathcal{R}_S$:

We expect that the activation takes place in localized clusters of the brain (gray-matter) with possibly sharp variations between them.

$\Longrightarrow$ We restrict a $3D$ conventional TV-regularization on the gray-matter.

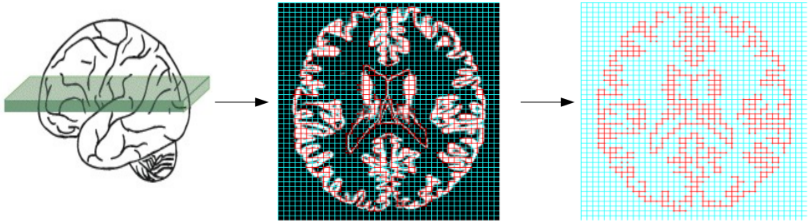

Conceptual 2D-view on gray-matter grid that is derived from the anatomical segmentation.

- Spatial regularization $\mathcal{R}_S$:

We expect that the activation takes place in localized clusters of the brain (gray-matter) with possibly sharp variations between them.

$\Longrightarrow$ We restrict a 3D conventional TV-regularization on the gray-matter.

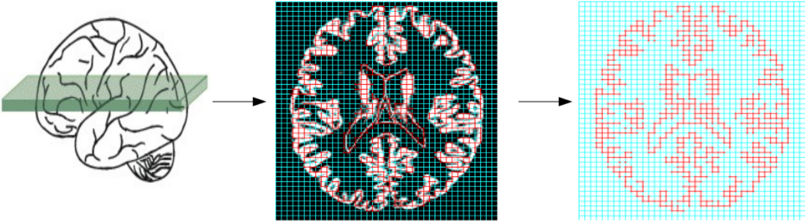

Conceptual 2D-view on gray-matter grid that is derived from the anatomical segmentation.

- At a time-point t: $TV^{GM}\{\mathbf{x}\}[t] = \sum_{v=1}^{N_x} \left(\sum_{u \in \mathcal{N}_v} \left(\mathbf{x}[v,t] - \mathbf{x}[u,t] \right)^2 \right)^{1/2}$,

where $\mathcal{N}_v$ denotes the set of neighbor voxels around v.

- Spatial regularization $\mathcal{R}_S$:

We expect that the activation takes place in localized clusters of the brain (gray-matter) with possibly sharp variations between them.

$\Longrightarrow$ We restrict a $3D$ conventional TV-regularization on the gray-matter.

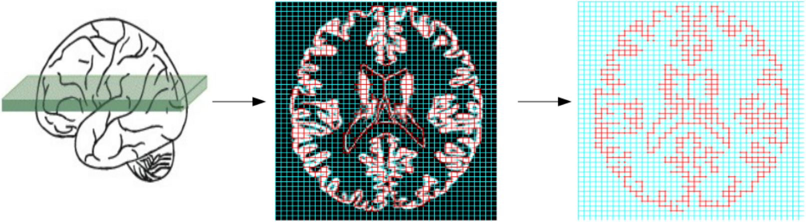

Conceptual 2D-view on gray-matter grid that is derived from the anatomical segmentation.

- At a time-point t: $TV^{GM}\{\mathbf{x}\}[t] = \sum_{v=1}^{N_x} \left(\sum_{u \in \mathcal{N}_v} \left(\mathbf{x}[v,t] - \mathbf{x}[u,t] \right)^2 \right)^{1/2}$,

where $\mathcal{N}_v$ denotes the set of neighbor voxels around v.

- Here again, the regularization should be applied for all time-points:

$$\mathcal{R}_S(\mathbf{x}) = \sum_{t=1}^{N_t} \lambda_S(t)\, TV^{GM}\{\mathbf{x}\}[t], \quad N_t \text{ : number of time-points}$$

We have, now, the variational formulation:

$$\widehat{\mathbf{x}} = \arg\min_{\mathbf{x}} \left\{ \frac{1}{2}||\mathbf{y}-\mathbf{x}||_2^2 + \overbrace{\sum_{t=1}^{N_t} \lambda_S(t)\, TV^{GM}\{\mathbf{x}\}[t]}^{\mathcal{R}_S} + \overbrace{\sum_{v=1}^{N_x} \lambda_T(v)\, ||\Delta_L\{\mathbf{x}\}[v]||_1}^{\mathcal{R}_T} \right\}.$$

We have, now, the variational formulation:

$$\widehat{\mathbf{x}} = \arg\min_{\mathbf{x}} \left\{ \frac{1}{2}||\mathbf{y} - \mathbf{x}||_2^2 + \underbrace{\overbrace{\sum_{t=1}^{N_t} \lambda_S(t)\, TV^{GM}\{\mathbf{x}\}[t]}^{\mathcal{R}_S} + \overbrace{\sum_{v=1}^{N_x} \lambda_T(v)\, ||\Delta_L\{\mathbf{x}\}[v]||_1}^{\mathcal{R}_T}}_{4D \text{ Structured TV}} \right\}.$$

We have, now, the variational formulation:

$$\widehat{\mathbf{x}} = \arg\min_{\mathbf{x}} \left\{ \frac{1}{2}||\mathbf{y}-\mathbf{x}||_2^2 + \underbrace{\overbrace{\sum_{t=1}^{N_t} \lambda_S(t)\; TV^{GM}\{\mathbf{x}\}[t]}^{\mathcal{R}_S} + \overbrace{\sum_{v=1}^{N_x} \lambda_T(v)\, ||\Delta_L\{\mathbf{x}\}[v]||_1}^{\mathcal{R}_T}}_{4D \text{ Structured TV}} \right\}.$$

Different operators on $\mathcal{R}_S$ and $\mathcal{R}_T$

We have, now, the variational formulation:

$$\widehat{\mathbf{x}} = \arg\min_{\mathbf{x}} \left\{ \frac{1}{2}||\mathbf{y}-\mathbf{x}||_2^2 + \underbrace{\overbrace{\sum_{t=1}^{N_t} \lambda_S(t)\, TV^{GM}\{\mathbf{x}\}[t]}^{\mathcal{R}_S} + \overbrace{\sum_{v=1}^{N_x} \lambda_T(v)\, ||\Delta_L\{\mathbf{x}\}[v]||_1}^{\mathcal{R}_T}}_{4D \text{ Structured TV}} \right\}.$$

Different operators on $\mathcal{R}_S$ and $\mathcal{R}_T \Longrightarrow$ Generalized forward-backward [Raguet et al. 2013]

We have, now, the variational formulation:

$$\widehat{\mathbf{x}} = \arg\min_{\mathbf{x}} \left\{ \frac{1}{2}||\mathbf{y}-\mathbf{x}||_2^2 + \underbrace{\overbrace{\sum_{t=1}^{N_t} \lambda_S(t)\; TV^{GM}\{\mathbf{x}\}[t]}^{\mathcal{R}_S} + \overbrace{\sum_{v=1}^{N_x} \lambda_T(v)\; ||\Delta_L\{\mathbf{x}\}[v]||_1}^{\mathcal{R}_T}}_{4D \text{ Structured TV}} \right\}.$$

Different operators on $\mathcal{R}_S$ and $\mathcal{R}_T \Longrightarrow$ Generalized forward-backward [Raguet et al. 2013]

Algorithm:

Input: Corrupted data $\mathbf{y}$, $(\omega_t, \omega_s) \in [0,1]^2$ with $\omega_s + \omega_t = 1$

Output: Estimate $\widetilde{\mathbf{x}}$

for $k = 1 : k_{max}$ **do**

1: $\mathbf{x}_t^k = \arg\min_{\mathbf{x}} \left\{ \frac{1}{2}||\mathbf{y}-\mathbf{x}||_2^2 + \mathcal{R}_T(\mathbf{x}) \right\}$,

2: $\mathbf{x}_s^k = \arg\min_{\mathbf{x}} \left\{ \frac{1}{2}||\mathbf{y}-\mathbf{x}||_2^2 + \mathcal{R}_S(\mathbf{x}) \right\}$,

3: $\mathbf{x}^k = \omega_t \mathbf{x}_t^k + \omega_s \mathbf{x}_s^k$

end for

$\widetilde{\mathbf{x}} = \mathbf{x}^{k_{max}}$

We have, now, the variational formulation:

$$\widehat{\mathbf{x}} = \arg\min_{\mathbf{x}} \left\{ \frac{1}{2}||\mathbf{y}-\mathbf{x}||_2^2 + \underbrace{\overbrace{\sum_{t=1}^{N_t} \lambda_S(t)\, TV^{GM}\{\mathbf{x}\}[t]}^{\mathcal{R}_S} + \overbrace{\sum_{v=1}^{N_x} \lambda_T(v)\, ||\Delta_L\{\mathbf{x}\}[v]||_1}^{\mathcal{R}_T}}_{4D \text{ Structured TV}} \right\}.$$

Different operators on $\mathcal{R}_S$ and $\mathcal{R}_T$ $\Longrightarrow$ Generalized forward-backward [Raguet et al. 2013]

Algorithm:

Input: Corrupted data $\mathbf{y}$, $(\omega_t, \omega_s) \in [0,1]^2$ with $\omega_s + \omega_t = 1$

Output: Estimate $\widetilde{\mathbf{x}}$

for $k = 1 : k_{max}$ **do**

1: $\mathbf{x}_t^k = \arg\min_{\mathbf{x}} \left\{ \frac{1}{2}||\mathbf{y}-\mathbf{x}||_2^2 + \mathcal{R}_T(\mathbf{x}) \right\}$,

2: $\mathbf{x}_s^k = \arg\min_{\mathbf{x}} \left\{ \frac{1}{2}||\mathbf{y}-\mathbf{x}||_2^2 + \mathcal{R}_S(\mathbf{x}) \right\}$,

3: $\mathbf{x}^k = \omega_t \mathbf{x}_t^k + \omega_s \mathbf{x}_s^k$

end for

$\widetilde{\mathbf{x}} = \mathbf{x}^{k_{max}}$

Solve steps 1 and 2 with a forward-backward algorithm (Fast Iterative Soft-Thresholding).

λ_t: Estimated from wavelet coefficients.

Test on simulated data

- FSL's simulation tool POSSUM

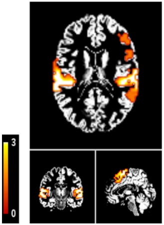

Activation map

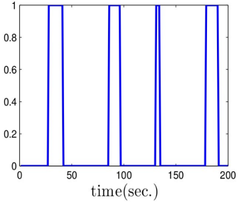

Experimental paradigm

Test on simulated data

- FSL's simulation tool POSSUM

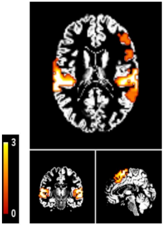

Activation map

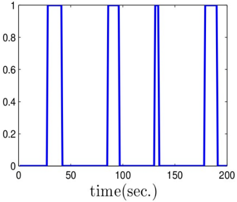

Experimental paradigm

$\Longrightarrow \varepsilon \sim \mathcal{N}(0,1)$, PSNR=8.49 dB.

Test on simulated data

- FSL's simulation tool POSSUM

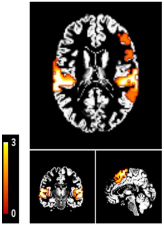

Activation map

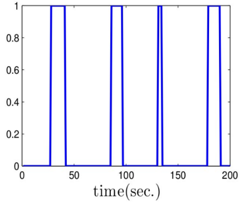

Experimental paradigm

$\Longrightarrow \varepsilon \sim \mathcal{N}(0,1)$, PSNR=8.49 dB.

TA (19.89 dB)

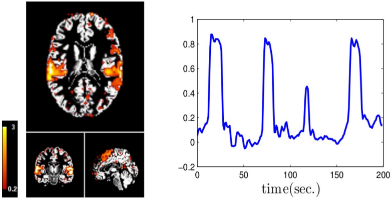

Atlas-free TA (22.50 dB)

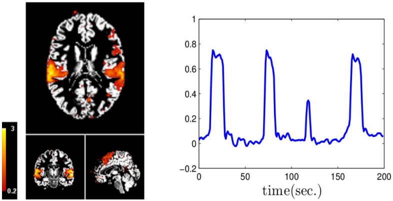

Reconstructed activity-related signal $\mathbf{x}$

Test on simulated data

- FSL's simulation tool POSSUM

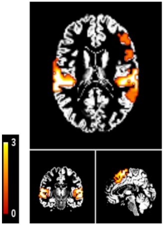

Activation map

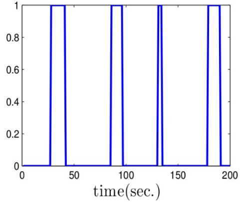

Experimental paradigm

$\Longrightarrow \varepsilon \sim \mathcal{N}(0,1)$, PSNR=8.49 dB.

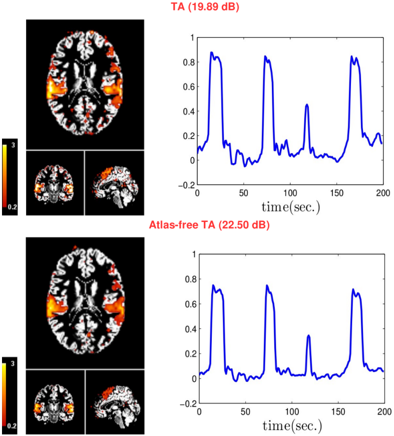

Reconstructed activity-related signal $\mathbf{x}$

- Less artifacts outside the activation regions $\Longrightarrow$ Better PSNR.

Test on simulated data

- FSL's simulation tool POSSUM

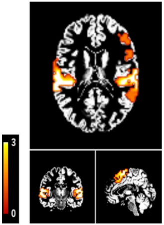

Activation map

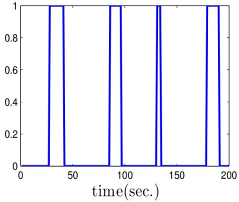

Experimental paradigm

$\Longrightarrow \varepsilon \sim \mathcal{N}(0,1)$, PSNR=8.49 dB.

TA (19.89 dB)

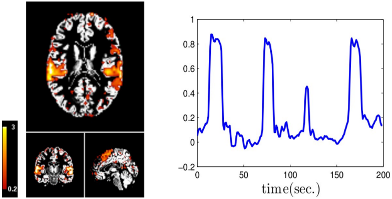

Atlas-free TA (22.50 dB)

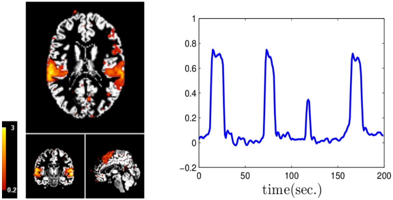

Reconstructed activity-related signal $\mathbf{x}$

- Less artifacts outside the activation regions $\Longrightarrow$ Better PSNR.
- Considerable gain in running time ($5h53min$ vs $4h30min$)

Test on real data

- Visual stimuli:

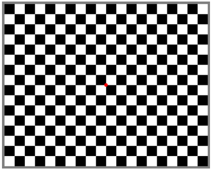

Flickering checkerboard.

Test on real data

- Visual stimuli:

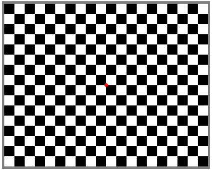

Flickering checkerboard.

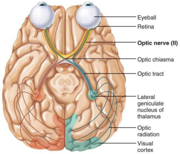

Visual cortex.

Test on real data

- Visual stimuli:

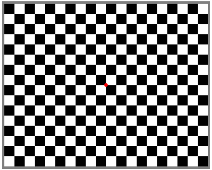

Flickering checkerboard.

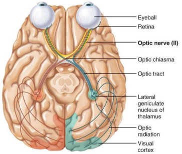

Visual cortex.

$\longrightarrow$ Rest periods disturbed by 9 visual stimuli of 1s at random time points.

Test on real data

- Visual stimuli:

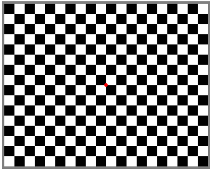

Flickering checkerboard.

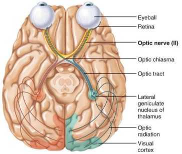

Visual cortex.

$\longrightarrow$ Rest periods disturbed by 9 visual stimuli of 1s at random time points.

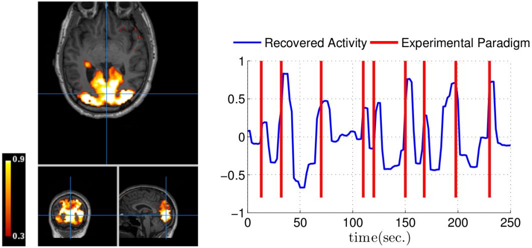

Recovered activity: (left) at a time point during the 2^{nd} activation, (right) within an activated area.

Test on real data

- Visual stimuli:

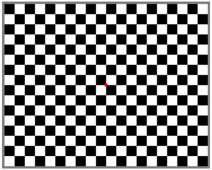

Flickering checkerboard.

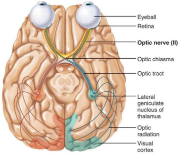

Visual cortex.

$\longrightarrow$ Rest periods disturbed by 9 visual stimuli of 1s at random time points.

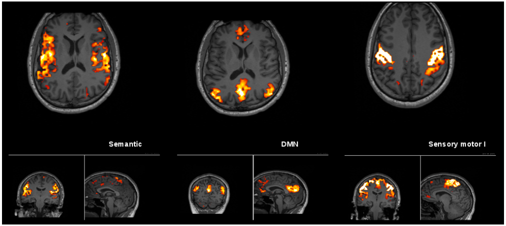

$\longrightarrow$ Richness of the activity during rest (networks).

Concluding remarks

$\longrightarrow$ What I didn't talk about:

- Evoked regions have high activity in the center that is vanishing towards white matter $\Longrightarrow$ drive the process by a probability map.

Concluding remarks

$\longrightarrow$ What I didn't talk about:

- Evoked regions have high activity in the center that is vanishing towards white matter $\Longrightarrow$ drive the process by a probability map.

$\longrightarrow$ Main perspectives:

- Applying the method to large datasets of resting-state fMRI to obtain innovation-driven co-activation patterns [Karahanoğlu & Van de Ville 2015].

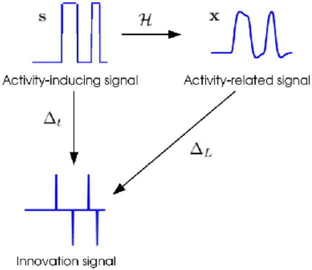

(Karahanoglu et al. 2015)

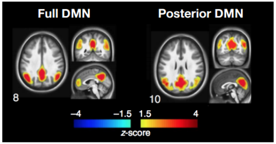

Concluding remarks

$\longrightarrow$ What I didn't talk about:

- Evoked regions have high activity in the center that is vanishing towards white matter $\Longrightarrow$ drive the process by a probability map.

$\longrightarrow$ Main perspectives:

- Applying the method to large datasets of resting-state fMRI to obtain innovation-driven co-activation patterns [Karahanoğlu & Van de Ville 2015].

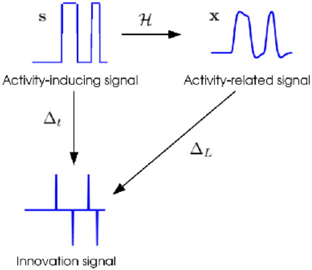

(Karahanoglu et al. 2015)

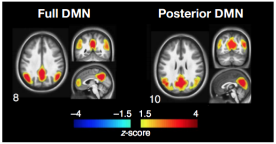

- Semi-blind deconvolution: Estimating the time-to-peak and dispersion of the hemodynamic function from data.

Thanks for your attention !

Any Questions ?